ANALYSIS OF THE EFFECTS OF NONLINEAR AMPLIFICATION ON TURBO CODING

PEDRO ENRIQUE SANTACRUZ

Department of Electrical and Computer Engineering

APPROVED:

_____

Bryan Usevitch, Ph.D., Chair

_____

Scott Starks, Ph.D.

_____

Roberto Osegueda, Ph.D.

_____

Pablo Arenaz, Ph.D.
Dean of the Graduate School

A

mi Mamá, mi Papá, Humberto y Gilberto

Gracias

ANALYSIS OF THE EFFECTS OF NONLINEAR AMPLIFICATION ON TURBO
CODING

by

PEDRO ENRIQUE SANTACRUZ

THESIS

Presented to the Faculty of the Graduate School of

The University of Texas at El Paso

in Partial Fulfillment

of the Requirements

for the Degree of

MASTER OF SCIENCE

Department of Electrical and Computer Engineering

THE UNIVERSITY OF TEXAS AT EL PASO

JULY 2006

Acknowledgements

First of all, I would like to thank Dr. Bryan Usevitch for all his guidance in the development of this thesis. Thank to his patience and commitment to delivery of good quality work, I obtained a very valuable experience.

Next, I would like to thank Dr. Eugene Grayver from the Aerospace Corporation for the idea for this thesis and for the unconditional support provided throughout the whole process. To the members of my committee for taking the time to participate in this process.

To all the people who contributed in many ways to the technical content of this thesis including Gopi Manne, Sashi Dharmannola, Irbis Gallegos, and Melissa Ruiz.

Also, a special thanks to Clarissa for her support and patience all along this process. Thanks for all the happiness and motivation.

Finally, thanks to my family for making my academic career possible and for all their love.

JULY 2006

Abstract

Satellite communications are used in a wide range of applications form military intelligence to weather forecast to commercial communications and entertainment. In special cases, satellite communication systems are required to perform with very low bit error rates. This requires the use of error coding techniques. In addition to that, in most cases satellite communication systems include nonlinear amplifiers to transmit from the satellite to the ground stations.

In this thesis, an analysis of the behavior of turbo coding in a nonlinear environment is presented. The relationship between coding gain and bit error rate at different power levels relative to saturation of a nonlinear amplifier is discussed. This analysis is performed using an end-to-end hardware platform. This hardware platform includes a digital modem, a radio frequency (RF) section, a nonlinear traveling wave tube amplifier (TWTA), and turbo coding ASIC. The analysis shows that coding gain is dependant on the power level of the nonlinear amplifier. In addition, the performance the 4+12 APSK modulation scheme on a nonlinear system using turbo coding is explored using a computer simulation of the hardware platform. The performance of the 4+12 ASPK modulation is compared to the performance of the 16QAM modulation scheme. The results show that the 4+12 APSK modulation scheme provides a better performance in a nonlinear system at low bit error rates.

Table of Contents

vii

List of Figures

Chapter 1

Introduction

1.1   Background and Motivation

In a communications system, performance is measured by sets of parameters related by some trade off relationship. Depending on the application of each system, these parameters take different priorities. In a satellite communications system, the parameters with the highest priority are power consumption, bit error rates, and bandwidth. Power consumption is an important factor to be considered because satellites obtain their power from solar cells. By their nature, solar cells do not provide as much power as could be provided by a station that was located on the ground, thus the importance of minimizing power usage. Acceptable bit error rates depending on the application must be reached in order for the system to be of any practical value. Some applications, such as military data communications require extremely low bit error rates, while others, like telephone communication, have more flexible requirements. Finally, given the vast amount of satellites orbiting the earth, all transmitting on the same portion of the frequency spectrum, bandwidth is a valuable resource.

In order to satisfactorily comply with as many of the previously mentioned parameters, different techniques are used at different levels of the communication system. To address the issue of power consumption, traveling-wave tube amplifiers (TWTA) are widely used in the satellite communications industry. TWTAs are primarily used because they are able to perform over a wide bandwidth, therefore providing a very desirable feature [Rod01]. On the other hand, these amplifiers behave in a nonlinear manner when operating at power levels close to saturation, which is the most effective region with regards to power consumption. This nonlinear behavior deteriorates the performance of the system and makes the analysis

of the expected behavior more complex. On the part of bit error rates, turbo coding algorithms are utilized to provide notably lower bit error rates with lower bit energy to noise power (E_b/N_o) ratios. It is for this reason that performance of communication systems in a nonlinear environment with coding algorithms is of particular importance and needs to be analyzed.

Simulating a satellite communication system on software alone is a nontrivial process due to the large number of parameters and the computationally intricate nature of signal coding algorithms. If we also add the estimation of nonlinearities to the complete system, the simulation requirements are increased significantly and the simulation becomes unpractical. A hardware platform such as the one used in this thesis makes the simulation of a satellite communication system practical and reliable.

In this thesis, a proof-of-concept hardware platform is used to provide a comprehensive analysis of the performance of turbo coding in a communication system with a nonlinear TWT amplifier. The metric of performance used to compare the different parameter scenarios is bit error rates at different E_b/N_o ratios. This analysis should provide a reliable guideline to estimate and/or evaluate the performance of systems with similar conditions.

1.2   Objective

The objective of this research is to create a comprehensive analysis of the effects of different modulation schemes, nonlinearities, and turbo coding algorithms on bit error rate performance in a communication system. A relationship between bit error rates (BER) of uncoded signals and BER of coded signals is examined. Also, the performance of a novel modulation scheme suited for nonlinear environments is offered. The digital modulation schemes that are taken into consideration are BPSK (binary phase-shift keying), QPSK (quadrature phase-shift keying), 8-PSK, 16-QAM (quadrature amplitude modulation), and 4+12 APSK (amplitude and phase-shift keying). The effect of nonlinearities is measured by including a TWTA with nonlinear behavior into the communication system. The TWTA at different

power levels provides different amounts of nonlinearity. In order to investigate how turbo coding influences the system, a Turbo Product Code Encoder/Decoder chip is introduced to the systems. A systematic procedure to combine the different sets of parameters is established and bit error rate graphs are obtained to compare the performance from each set and established the effects of each parameter. Coding gain produced by the turbo coding algorithm is also analyzed under the different parameter combinations.

1.3   Outline

This thesis is divided into six chapters. The introduction is included in Chapter 1 and consists of the motivation, the objective, and this outline. Chapter 2 gives an explanation of the different types of digital modulation schemes implemented and explains how nonlinearities affect these modulation schemes. Chapter 3 provides background information on Turbo Coding. Chapter 4 describes the system utilized to perform the work presented in this thesis. Chapter 5 provides the experimental procedure of the work performed and presents its results. Chapter 6 consists of the conclusions and suggestions for future work.

Chapter 2

Digital Modulation Schemes and Nonlinear Amplification

2.1 Digital Modulation

A digital communication system is defined as a system in which the source signal to be transmitted is a sequence of binary digits. This binary sequence is then modulated, sent through a communication channel, demodulated, and finally converted back to its original form of a sequence of binary digits [Pro01]. Digital modulation refers to the process of mapping the digital information from the source sequence into analog waveforms that can be transmitted through a communication channel. This mapping in generally performed by taking $k = log_2 M$ bits from the source sequence and mapping them to one of the M different waveforms in a waveform space. Each block of k bits is called a symbol. The waveforms can then be represented by vectors in a signal space. The plotting of these vectors in the signal space is called the signal space representation or constellation.

There are three main types of digital modulation schemes used in this thesis. They are pulse amplitude modulation (PAM), also called amplitude-shift keying (ASK), phase modulation, also called phase-shift keying (PSK), and quadrature amplitude modulation (QAM).

2.1.1 Amplitude-Shift Keying

Pulse-amplitude-modulated signals produce a one-dimensional analog signal that can be represented as

$$s_m(t) = Re[A_m g(t) e^{j2\pi f_c t}] = A_m g(t) \cos(2\pi f_c t).$$

where A_m is one of the M amplitudes designed to create the M different waveforms. It can be said that

$$A_m = (2m - 1 - M)d$$

where $m = 1, 2, ..., M$ and d the distance between each one of the points. Some examples of the signal space representation of PAM signals are presented in Figure 2.1
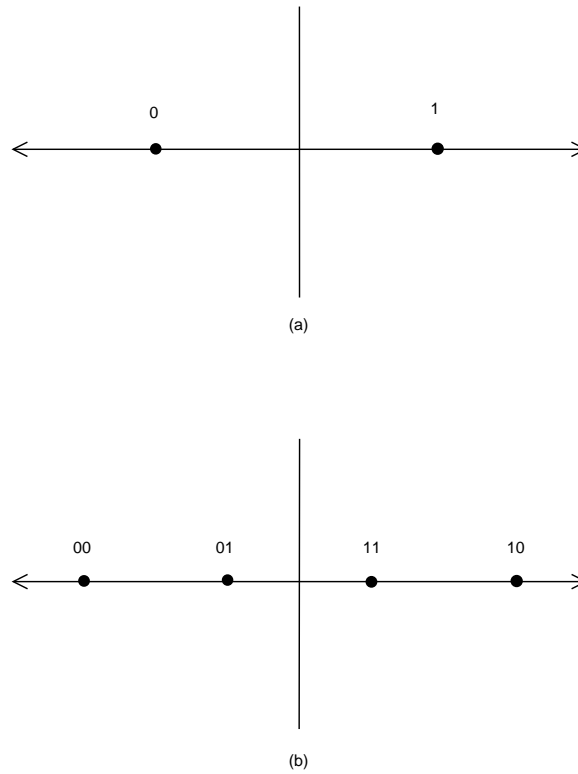

Figure 2.1: Signal space Representation of PAM. (a) M = 2, (b) M = 4

2.1.2 Phase-Shift Keying

In phase modulation, the source information is encoded into the analog waveforms by letting the information symbols determine the phase of the analog waveform. The waveforms can be described as follows

$$
\begin{aligned}
s_m(t) &= Re[g(t)e^{j2\pi(m-1)/M}e^{j2\pi f_c t}] = g(t)\cos[2\pi f_c t + \frac{2\pi}{M}(m-1)] \\
&= g(t)\cos\frac{2\pi}{M}(m-1)\cos 2\pi f_c t - g(t)\sin\frac{2\pi}{M}(m-1)\sin 2\pi f_c t,
\end{aligned}
$$

where $m = 1, 2, , M$ and M is the number of distinct waveforms. Therefore, the phase for the carrier that is being modulated by $g(t)$ is $2\pi(m-1)/M$.

In a signal space, all possible waveforms of this form span a space of two dimensions, and therefore, can be represented as a linear combination of two orthogonal signal waveforms. Figure 2.2 shows the vector representations of PSK with different values of M.

2.1.3 Quadrature Amplitude Modulation

Quadrature amplitude modulation is the result of mapping two different source symbols into two different carrier namely $\cos 2\pi f_c t$ and $\sin 2\pi f_c t$. That is, we apply the same procedure as amplitude-shift keying but in two different carrier that are orthogonal therefore creating a two-dimensional signal space. The quadrature amplitude signal can be described as follows

$$
\begin{aligned}
s_m(t) &= Re[(A_{mc} + jA_{ms})g(t)e^{j2\pi f_c t}] \\
&= A_{mc}g(t)\cos 2\pi f_c t - A_{ms}g(t)sin2\pi f_c t,
\end{aligned}
$$

where A_{mc} and A_{ms} are the two different symbols carrying information for the source sequence.

It is important to note that, as in the case of amplitude modulation, each one of the waveforms in the signal space of QAM has a different energy except in the case of 4-QAM.
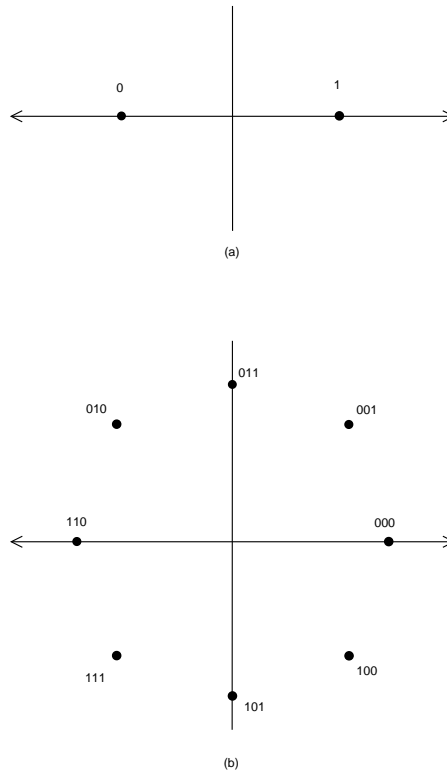
Figure 2.2: Space Representation of PSK. (a) M = 2, BPSK; (b) M = 8, 8-PSK

The energy of the waveform is proportional to the norm of the vector in the signal space. Figure 2.3 displays examples of signal space representations of QAM modulations.

2.2 Nonlinear Amplification

One of the components of the communication system used for this work is an amplifier that exhibits nonlinear behavior. This nonlinear behavior of amplifiers is much more prevalent when the amplifier is operated close to the saturation level [Rod01]. At low power levels of the input signal, the amplifier acts as a linear amplifier, that is, a specific change of decibels at the input is represented by the same change in decibels at the output. This behavior can be expressed as follows. Given that the amplifier is linear and $x_1(t)$ and $x_2(t)$ are inputs to the system and $gy_1(t)$ and $gy_2(t)$ the corresponding outputs then the input

$$Ax_1(t) + Bx_2(t)$$

will give the output

$$gAy_1(t) + gBy_2(t),$$

where A and B constants and g is the gain of the amplifier. In a logarithmic scale, the A and B multiplicative constants translate into additive constants. When the previous equations do not hold, then the amplifier is said to be nonlinear and this is often denoted as AM/AM nonlinearity.

There exists another characteristic associated with nonlinear amplifiers called AM/PM conversion. This occurs when a change in the power level of the input signal results in a change in the phase of the signal. Similar to AM/AM nonlinearity, AM/PM conversion has its greatest effect when the amplifier is operated closer to the saturation point.

Keeping in mind the two types of effects that the nonlinear amplifier has on the input signal, consider a constellation where the waveform do not have the same power, as in the case of 16-QAM. When this constellation is applied through a nonlinear amplifier, the waveforms with the highest power level will be more affected by the nonlinearity and therefore are more susceptible to lose their constellation form. In a modulation scheme where all waveforms have the same power, nonlinearities will affect all points in the same way, thus having a greater probability of retaining its constellation form. Figure 2.4 shows the effects of nonlinearities on two different modulation schemes.

As depicted in Figure 2.4 the four outermost points in the 16-QAM constellation are heavily affected by the nonlinear effects of the amplifier. The points not only tend to come inside towards the center of the plot, but they also rotate to the sides because of the AM/PM conversion. The inner four points of the 16-QAM constellation also exhibit the rotation due to the phase distortion. In contrast, the 8-PSK constellation is much less affected and only displays an elongation of the clouds of noise around the expected location of the data points.
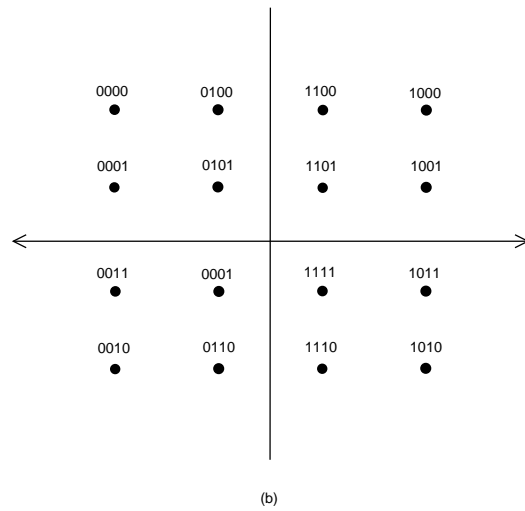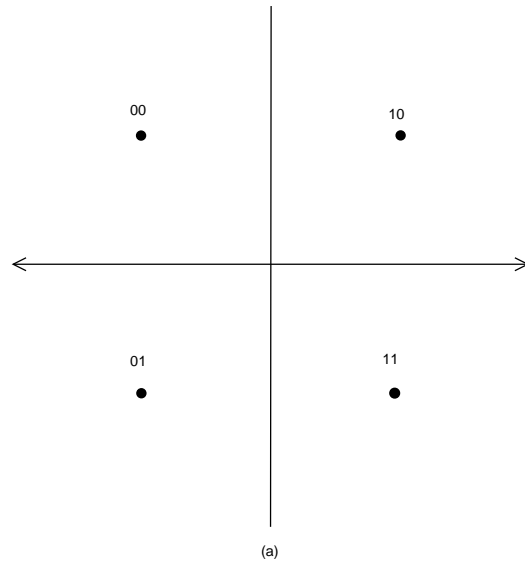
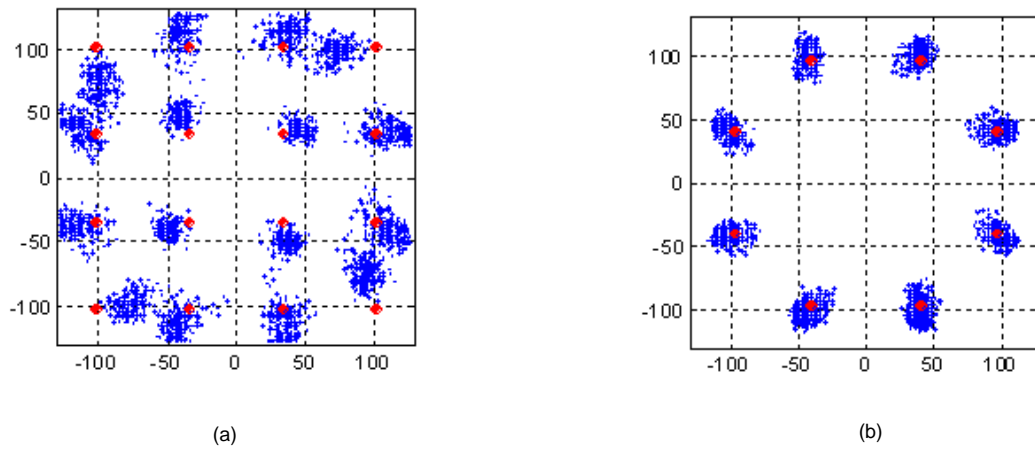Figure 2.3: Signal Space Representation of QAM. (a) M = 4, 4-QAM; (b) M = 16, 16-QAM

Figure 2.4: Effects of nonlinearities on (a) 16-QAM and (b) 8-PSK

Chapter 3

Turbo Coding

3.1   Error Correction Coding

In a digital communication system, the main objective is to transmit and receive information in a fast and reliable manner. In 1948, Shannon mathematically proved that by preparing, or encoding, information in a specific way, it is possible to conduct error-free transmission of information over a noisy channel as long as the rate of the information is not greater than the capacity of the channel [Sha48]. Research has since been applied to the development of a coding process that will reach the Shannon limit. In digital communications, error correction coding refers then to the process of encoding an information bit sequence in order to be able correct errors produced by a noisy channel when the received information is decoded.

There are two main types of error correction codes used today: block codes and convolutional codes [LJ04]. Both types of coding take the input information sequence in blocks of size k and produce a coded sequence of size n. The main difference between block codes and convolutional codes is that convolutional codes depend not only on the message being processed in the current time frame but also on previous messages. Therefore, convolutional codes are said to have memory. The rate of both types of codes is defined as $R = k/n$, the ratio of information bits to total bits of the encoded message.

3.2   Turbo Coding Algorithm

Turbo coding was first introduced in 1993 by Berrou, Glavieux, and Thitimajshima [CBT93]. This type of coding performs close to the channel limit due to two important factors. Primar-

11

ily, turbo coding has randomlike properties in the way it develops its codes. Also, because the code is structured in some ways regardless of its randomlike behavior, the decoding algorithm can be implemented in an iterative manner based on soft-decisions [LJ04], [VY00]. The turbo coded sequence consists of two or more simple constituent codes. These constituent codes include blocks that have been coded at different points of the systems with the introduction of a pseudorandom interleaver. This section will explain the turbo coding process, the decoding process, and the theoretical performance of the code through an AWGN channel.

3.2.1 Encoding

As previously mentioned, creating two or more constituent codes that have a randomlike behavior is essential for the proper performance of turbo codes. This constituent codes are probabilistically independent from each other and they will provide information that will result in a better detection of the encoded signal. The basic approach to achieving this goal is described in Figure 3.1.

In the case of Fig. 3.1, the vector $\mathbf{v}^{(0)}$ is sequence of bits of the original message of length k plus some termination bits to make them length K. The vector $\mathbf{v}^{(1)}$ is the first constituent code that has been encoded using a convolutional encoder. The vector $\mathbf{v}^{(2)}$ is the second constituent code that has been processed by a pseudorandom interleaver and then encoded with a convolutional encoder. Typically, all constituent codes are obtained using the same encoder, but the use of different encoder might produce better performance [LJ04]. Finally, the three constituent codes are combined to create a single sequence of the following form: $\mathbf{v} = (\mathbf{v}_0^{(0)}, \mathbf{v}_0^{(1)}, \mathbf{v}_0^{(2)}, \mathbf{v}_1^{(0)}, \mathbf{v}_1^{(1)}, \mathbf{v}_1^{(2)}, ..., \mathbf{v}_{K-1}^{(0)}, \mathbf{v}_{K-1}^{(1)}, \mathbf{v}_{K-1}^{(2)})$. In this example, there is only one interleaver and two encoders for a total of three constituent codes. More interleavers and encoders can be added so that more parity bits are added by paying the cost of lower coding rates. An encoding system with more than three constituent codes is often called a *multiple turbo code*.

The overall coding scheme of turbo codes is known as *parallel concatenated convolutional*
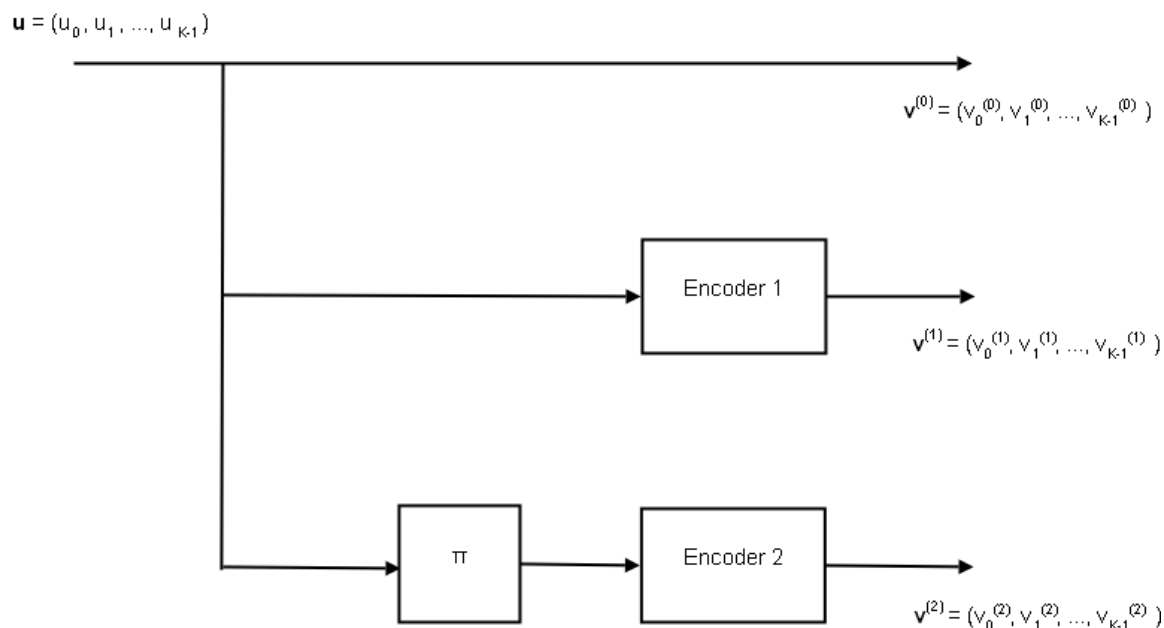
$$\mathbf{u} = (u_0, u_1, ..., u_{K-1})$$

$$\mathbf{v}^{(0)} = (v_0^{(0)}, v_1^{(0)}, ..., v_{K-1}^{(0)})$$

Encoder 1

$$\mathbf{v}^{(1)} = (v_0^{(1)}, v_1^{(1)}, ..., v_{K-1}^{(1)})$$

π

Encoder 2

$$\mathbf{v}^{(2)} = (v_0^{(2)}, v_1^{(2)}, ..., v_{K-1}^{(2)})$$

Figure 3.1: Basic diagram of turbo encoding process

code (PCCC) [VY00]. Concatenated codes typically perform in a serial manner in which an input block is encoded by the first encoder, interleaved, and then encoded again by the second encoder. Turbo codes, on the other hand, act on different versions of the same input block at the same time using different encoders and then produce a multiplexed sequence of parity bits. Given that the interleaver has pseudorandom characteristics, an input block of low weight will produce a high weight output when put through the turbo encoder of Figure 3.1. This shift of the weight spectrum from low weight to high weight creates a random-like distribution of the codes created, and is thus responsible for the significant increase in performance at lower BERs.

3.2.2 Decoding

Optimum performance of turbo codes is achieved when the codes are decoded using the maximum a posteriori (MAP) method, also known as a posteriori probability (APP). Nevertheless, implementing the MAP algorithm to decode a message encoded using the encoding

procedure described in Section 3.2.1 would be extremely complex, making the process impractical. The idea in decoding turbo codes is to reduce the complexity by creating an iterative procedure in which each step is decoded with a suboptimal algorithm. The iterative process converges then to the result obtained with the optimum decoding algorithm.

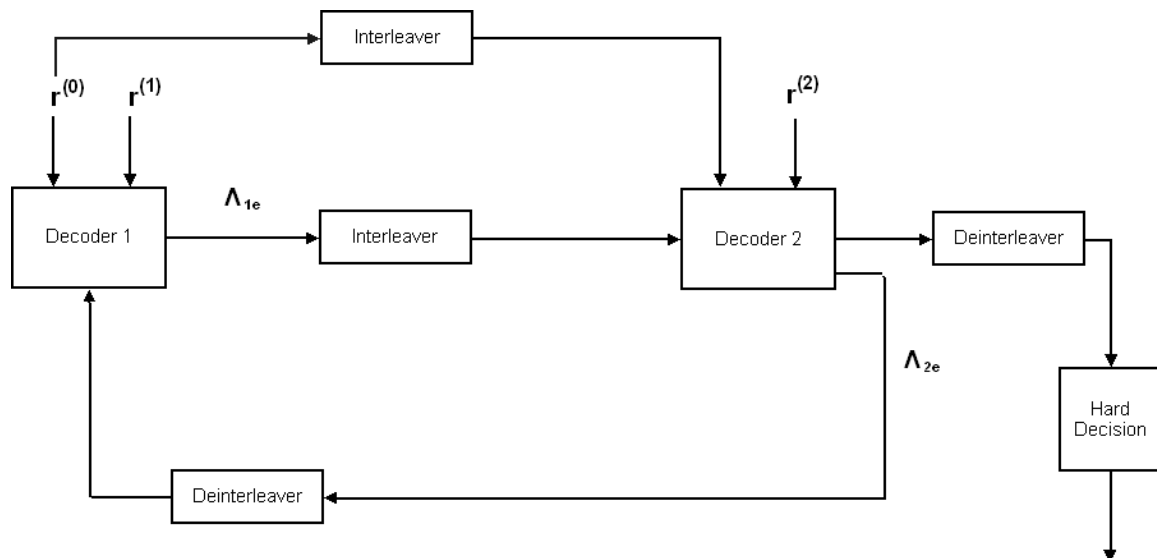Figure 3.2 illustrates the basic concept of the iterative turbo decoding algorithm.

Figure 3.2: Iterative turbo decoding algorithm

In Figure 3.2, $\mathbf{r^{(0)}}$, $\mathbf{r^{(1)}}$, and $\mathbf{r^{(2)}}$ are the received vectors resulting from the transmission of vectors $\mathbf{v^{(0)}}$, $\mathbf{v^{(1)}}$, and $\mathbf{v^{(2)}}$ through a communication channel with additive white gaussian noise (AWGN), respectively. The received vectors are expected to have been affected by noise and using a hard decision algorithm would result in many errors. $\mathbf{\Lambda_{1e}}$ and $\mathbf{\Lambda_{2e}}$ are the extrinsic a posteriori log-likelihood ratio resulting from the soft decision Decoder 1 and Decoder 2, respectively. The log-likelihood ratio is defined as follows:

$$
\begin{aligned}
\mathbf{\Lambda}(\nu_\mathbf{l}) &= \ln \frac{P(\nu_l = +1|r_l^{(0)})}{P(\nu_l = -1|r_l^{(0)})} = \ln \frac{e^{-(E_b/N_0)(r_l^{(0)}-1)^2}}{e^{-(E_b/N_0)(r_l^{(0)}+1)^2}} \\
&= -\frac{E_b}{N_0}\{(r_l^{(0)} - 1)^2 - (r_l^{(0)} + 1)^2\} + \ln \frac{P(\nu_l = +1)}{P(\nu_l = -1)}
\end{aligned}
$$

14

where $l = 1, 2, , k$ is the number of the bit being decoded, E_b is the bit energy, and both ν_l and r_l have been normalized by a factor of $\sqrt{E_b}$. Notice that the second part of the last equation is the log-likelihood ratios of the a priori probabilities of ν_l. Therefore, in order for the decoders to calculate the a posteriori log-likelihood ratios, they need to know the a priori probabilities of ν_l. The diagram in Figure **??** depicts how the extrinsic a posteriori log-likelihood ratios of each one decoder, after interleaving or deinterleaving, are used as the a priori log-likelihood ratios for the other decoder. To begin the process we assume equal a priori probabilities of $\nu = 1$ and $\nu = -1$, so the log-likelihood ratio is 0. Each time, the decoders will provide better and better a posteriori values, so with each iteration, the system will be closer to decoding the bit that was actually transmitted. After a number of iterations, no more significant improvements will be obtained and the iterative system should be stopped and a final hard decision is made. It is important to notice the assumptions that have been made. First, it is assumed that this iterative turbo decoding algorithm keeps improving with each iteration. Second, it is also assumed that this system provides a converging result and that no more improvements are made after some point. The theoretical bases for these claims are discussed in [HG02], [BM96], and [tB01].

3.3 Performance of Turbo Codes

The measure used to evaluate the performance of turbo codes is the probability of bit error $P_b(E)$ with respect to the ratio of bit energy to noise (E_b/N_0). There are many factors that affect the performance of turbo codes and here are the most notable ones:

- Interleaver (block) size

- Number of iterations

- Puncturing of component codes

- Type of decoder

Considering each factor individually, as the interleaver block size increases, the performance of turbo codes also increases (i.e. the bit error rate is decreased for a specific E_b/N_0). Also, as the number of iterations increases, performance increases, until the threshold where iterations do not provide further improvement is reached. Puncturing the codes will provide a better coding rate but will decrease the performance of the code. Regarding the type of decoder, the maximum a posteriori (MAP) decoder provides the best performance for the codes.

3.3.1 Coding Gain Definition

In order to standardize the way in which coding performance is evaluated, a metric that is generally accepted is the coding gain. Coding gain is defined as the difference in dB of signal-to-noise ratio required to obtain a specific bit error rate. Figure 3.3 shows an example of coding gain of 3 dB at 10^{-6} BER.
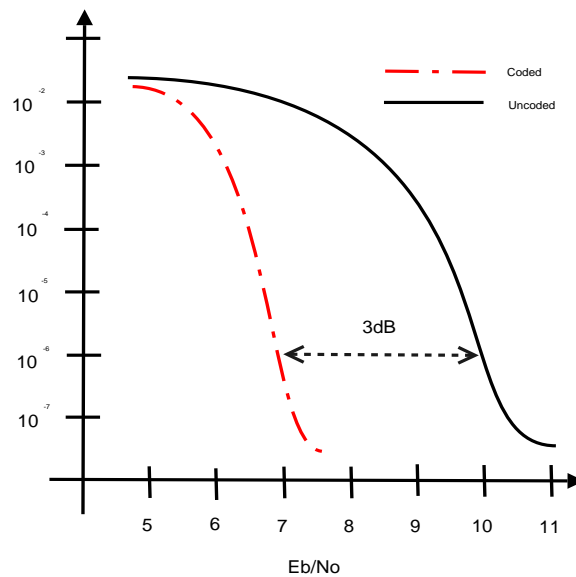

Figure 3.3: Coding Gain

Since the work included in this thesis deals primarily with the performance of turbo codes

in a nonlinear environment, a very particular behavior appears in the BER plots obtained. This behavior shows up as an error floor (or what can be called a "horizontal asymptote") in medium bit error rates on the uncoded curves. Since the coded curves reach a lower bit error rate, the traditional difference in dB at lower BER does not exist. For this reason, a vertical mapping of coded BER to uncoded BER for a specific E_b/N_0 is proposed as an alternative to coding gain. This mapping still possesses all the information that the traditional coding gain provides. Figure 3.4 characterizes how this mapping is defined.
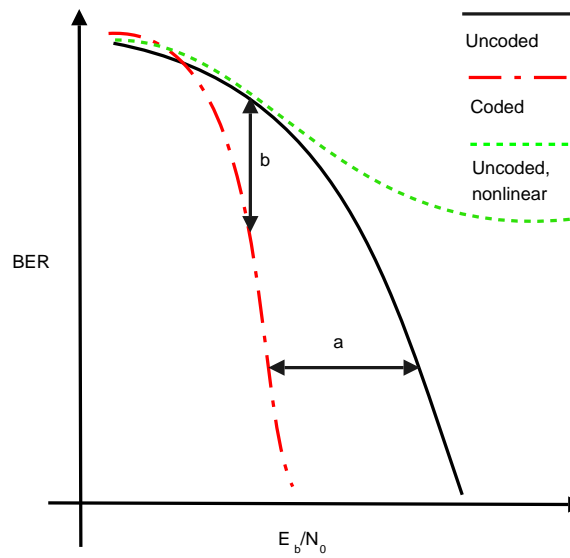

Figure 3.4: a) Traditional coding gain, b) vertical mapping

Chapter 4

System Used for Experimental Procedure

4.1 System

Analyzing the behavior of turbo coding through a nonlinear system can be performed by simulating the complete communication system using complex software models of each of the components. The main disadvantage to this approach is the amount of time required to obtain the desired simulation, thus making this approach unpractical in many cases. Also, it is important to keep in mind that a software simulation is only an approximation of the behavior of the system that will ultimately be implemented in hardware. A hardware platform allows this analysis to be done in a much more efficient and reliable manner. This section will describe the system utilized to perform the work presented in this thesis.

4.1.1 GOES-R System

The hardware system used is a proof-of-concept platform that was developed as a risk-reduction stage in the development of the transmitter and receiver sub-systems for the next generation Geostationary Operational Environmental Satellites R-series (GOES-R) [GS06]. This communication system includes a digital data source, a modem, a turbo encoder/decoder chip, a radio frequency (RF) section, an external noise source, and a personal computer (PC) for user control. Figure 4.1 presents an overall overview of the major components of the system.
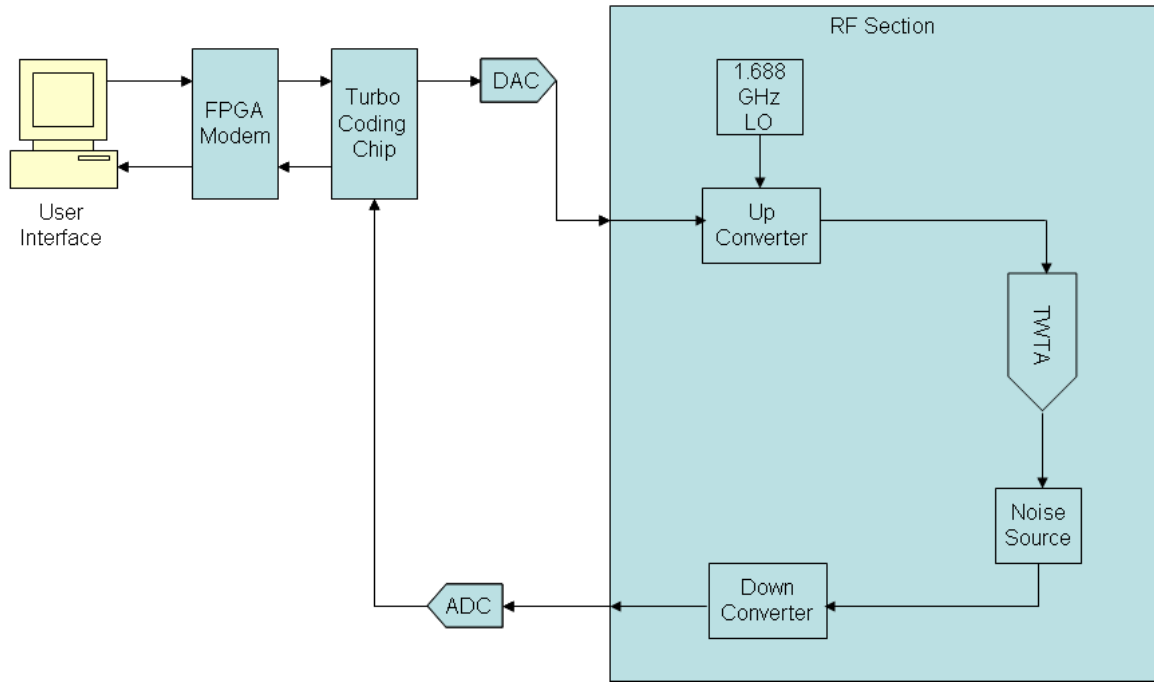
Figure 4.1: Overall System Overview

4.1.2 TWTA

The traveling wave tube amplifier (TWTA) included in this system could be considered the main component of the setup since it is the source of the nonlinearities being analyzed. The TWTA is a space-qualified amplifier manufactured by Boeing and it is comparable to amplifiers that are currently put in flight in operational satellites. It is rated for an output power of 150W (52 dBm) at L-band (i.e. 390 MHz to 1.55 GHz). As with most high power amplifiers, this TWTA exhibits AM/AM and AM/PM distortion. AM/AM distortion refers to the behavior where a linear change in power level at the input of the amplifier does not correspond to a linear change in the power level at the output. AM/PM distortion occurs when a change in the input power level results in a change in phase at the output [Rod01]. Both of these types of distortion typically happen when the amplifier is operated close to the saturation level.

It is important to define the units to be used when referring to the power level of the

amplifier. The amplifier has a power level at which it saturates and no longer performs as expected. Because most of the nonlinear behavior of the amplifier occurs close to that saturation level, our power level units, denoted dBsat, are defined with respect to that level. A dBsat refers to a decibel unit below the saturation level. This convention in commonplace in nonlinear amplification contexts, including [GS06].

In order to mitigate the effects of severe nonlinear behavior of the TWTA, a commercially available linearizer is introduced to the system. This is common practice in operational satellite systems. Nonetheless, even with the presence of the linearizer, the performance of the system is nonlinear. The performance of the TWTA, with and without the linearizer, is described in Figure 4.2.
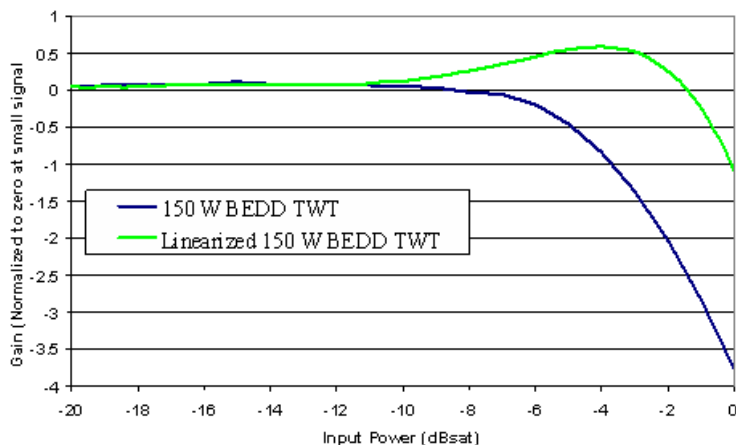

Figure 4.2: AM/AM Performance of TWTA

Figure 4.2 shows that as the input power level to the amplifier starts approaching the saturation point, the normalized gain start deviating from 0 and starts decreasing rapidly at around the 10 dBsat mark. The linearizer improves the performance, but it is shown that the expected consistent line at 0 is not obtained. Figure 4.3 shows a similar behavior in terms of phase distortion, except the deviation from the desired starts appearing at about the 16 dBsat mark.
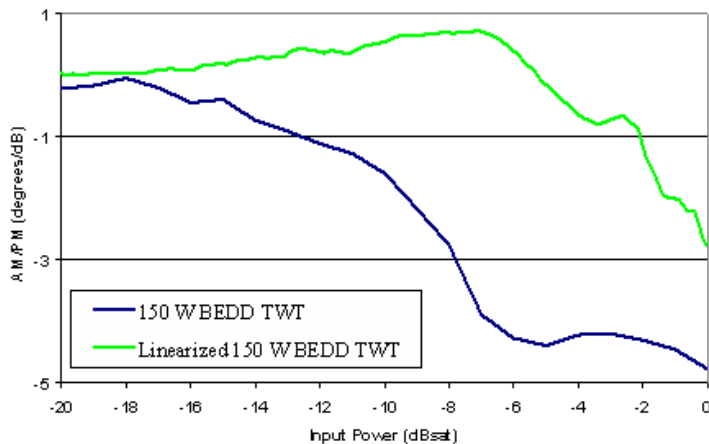
Figure 4.3: AM/PM Performance of TWTA

4.2 User Interface and Modem

The system provides a software-defined radio (i.e. it uses software to modulate and demod-
ulate radio signals [MDA03]) in the form of a graphical user interface (GUI) that allows
the user to control many parameters of the communication system in real time. Table 4.2
presents some of the parameters available to the user for modification.

The system performs all modulation and demodulation algorithms using a Xilinx FPGA
(field programmable gate array) Virtex-II 6000 [XIL05] and [GD05]. Table 4.2 shows the
modulations that are supported by the modem. Bit error rates obtained from the imple-
mentation of this system were compared to the expected theoretical bit error rates through
a AWGN channel and the results showed a 0.6 dB implementation loss at very low BER
(10^{-9}).

4.2.1 Turbo Coding

Implementation of turbo coding is one of the parameters that can be modified in real time on
the hardware platform. The turbo coding and decoding algorithms are executed on an AHA
turbo coding ASIC (application-specific integrated circuit). The AHA ASIC uses Extended

Table 4.1: Modem parameters available for editing

Category	Capabilities
Modulations	BPSK, QPSK, 8-PSK, 16-QAM, 32 QAM, 64-QAM
	Arbitrary constellation, up to 64-ary
	T offset option
	FSK, 4-FSK, 8-FSK with programmable h, MSK, GMSK
Symbol Rate	$\leq$ 10 MSPS for linear modulations
	$\leq$ 5 MSPS for FSK type modulations
Data Rate	$\leq$ 20 Mbps using QPSK, $\leq$ 60 Mbps using 64-QAM
Pulse shape	Square-root raised cosine ($\alpha = 0.35$)
	Programmable 212-tap filter
	Gaussian filter for GMSK
Digital freq synthesis	SFDR $>$ 60 dBc
	0.1 Hz resolution
Coding	Turbo Product Codes (up to 16 Kb)
	Code rates from 0.25 to 0.99
Implementation Loss (digital)	$\leq$ 0.4 dB for linear modulations
	$\leq$ 2 dB for FSK type modulations
Mixed signal	DAC: 16 bit, 400 MSPS; ADC: 12 bit, 125 MSPS

Hamming Codes in two dimensions. Even though the ASIC has the capability to perform in three dimensions, that option is not used in this hardware platform because it takes more time to perform that process. Additionally, in this experimental procedure, turbo coding was implemented at a rate of $r = 0.954 : (64, 63)x(64, 62)$. This means that in one dimension, 63 bits out of 64 bits were data bits and in the other dimension 62 out of 64 bits were data bits. After coding, the bits are arranged in a $64x64$ matrix [Com05].

The turbo coding AHA ASIC has a large number of parameters that can be manipulated to achieve the best performance. Some of these parameters include the number of iterations, enabling helical interleaving, the block size, enabling code shortening, addition of feedback in any of the dimensions, and the number of quantization bits. For this work, all these parameters are set to give the best performance (i.e. a lower bit error rate at a specific E_b/N_0) and are not changed throughout the course of the experimental procedure.

With respect to the turbo coding, the options that are of relevance to this work are the implementation of the turbo code and the modulation scheme being used.

4.2.2 RF Section

A radio frequency (RF) section is included in the system to approximate its performance to a real satellite communications system. The RF section consists of an up-converter with a center frequency of 1.688 GHz that moves the baseband signal to that part of the spectrum. It also includes a calibrated external noise source that adds noise to channel after the TWTA. Finally, there is a down-converter using the same 1.688 GHz to bring back the passband signal with noise back to baseband.

Figure 4.4 displays the hardware platform setup in the lab including the GUI to the right, TWTA to the left, and RF section towards the bottom.
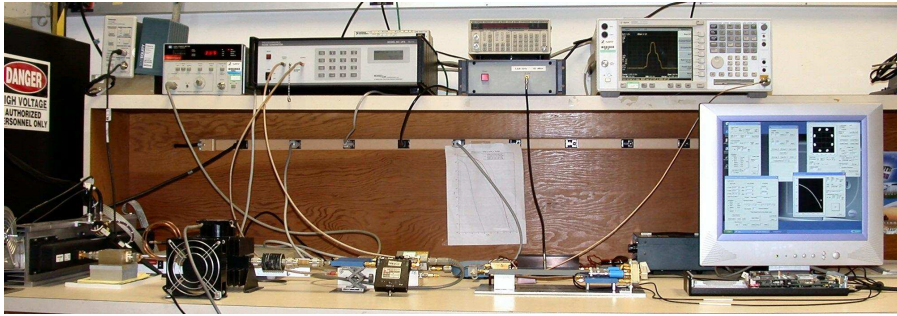
Figure 4.4: GOES-R System

Chapter 5

Effects of Nonlinear Amplification on Turbo Coding

This chapter discusses the results obtained from the work performed in this thesis as well as the details of the procedure used to obtain such results. The chapter is divided into sections that discuss the methodology, the results obtained from the implementation on the hardware system, and the results of the software simulations.

5.1 Methodology and Experimental Procedure

The main objective of this thesis is to develop a good understanding of the how the performance of turbo coding is affected by the presence of a nonlinear amplifier and the use of different modulation schemes. Therefore, the first step in the experimental process is to develop a wide and varied set of performance curves. The metric used to evaluate the performance of the system is bit error rate (BER) with respect to signal-to-noise ratio (E_b/N_0). Because of this metric, the set of performance curves developed consists of BER curves with different parameters established at different states. The parameters and their possible states are detailed on Table 5.1.

The set of performance curves provides a source of analysis of the behavior of these parameters with respect to each other. From this set of curves the possibility of predicting the behavior of turbo coding under nonlinear conditions having as a reference the behavior of turbo coding under linear conditions for a specific modulation scheme is addressed. In addition to this, the relation of the other parameters and the possibilities of other types of predictions are analyzed.

Table 5.1: Parameters to be analyzed

Parameter	Possible Status
Nonlinearity	**Feedback** (Linear) or **Nonlinear** (from 3.8 dBsat to 0.8 dBsat)
Turbo Coding	**Enabled** or **Disabled**
Modulation Scheme	**8PSK** or **16QAM** (**4+12 APSK** on software simulation)

The analysis of the set of curves consists of the following. First, a relationship, or lack thereof, between the uncoded BER plot and the coded BER plot with a specific modulation scheme is established. Also, the effect of different amounts of nonlinearity (in power levels measured in dBsat) on different modulation schemes is examined. Once the analysis of the curves obtained in the hardware platform is completed, the next step is to perform some computer simulations using MATLAB. These computer simulations allow for the analysis of the performance of the 4+12 APSK modulation scheme. The need for computer simulations lies in the fact that the 4+12 APSK modulation scheme is not supported by the turbo coding chip in the hardware platform. Results for the expected coded performance of the 4+12A APSK constellation under linear conditions have been previously published [15, 16] and the purpose of these simulations is to obtain the expected performance of 4+12 APSK under nonlinear conditions.

5.2   Set of BER Curves

The set of BER curves presented in Figures 5.1 - 5.6 is obtained using the hardware platform described in Chapter 4 because of its reliability and fast delivery. In order to obtain each one of the data lines on the previous plots there are several important points to be considered. First, all plots are obtained from the same system with all other parameters constant except the ones specified as a change (in this case modulation scheme, amount of dBsat, or enabling of turbo code). Each one of the points in the BER plot is obtained by continuously
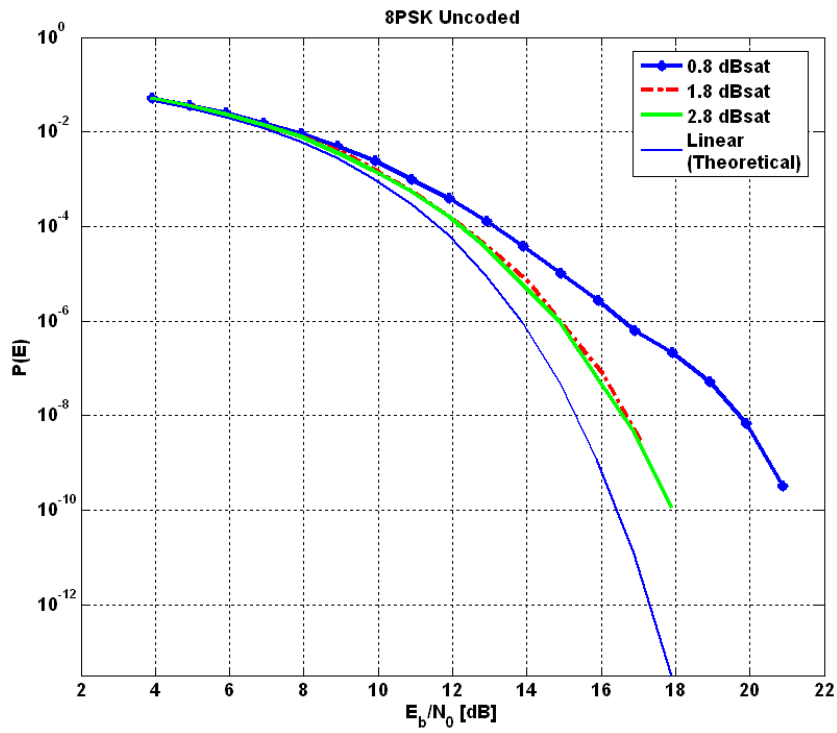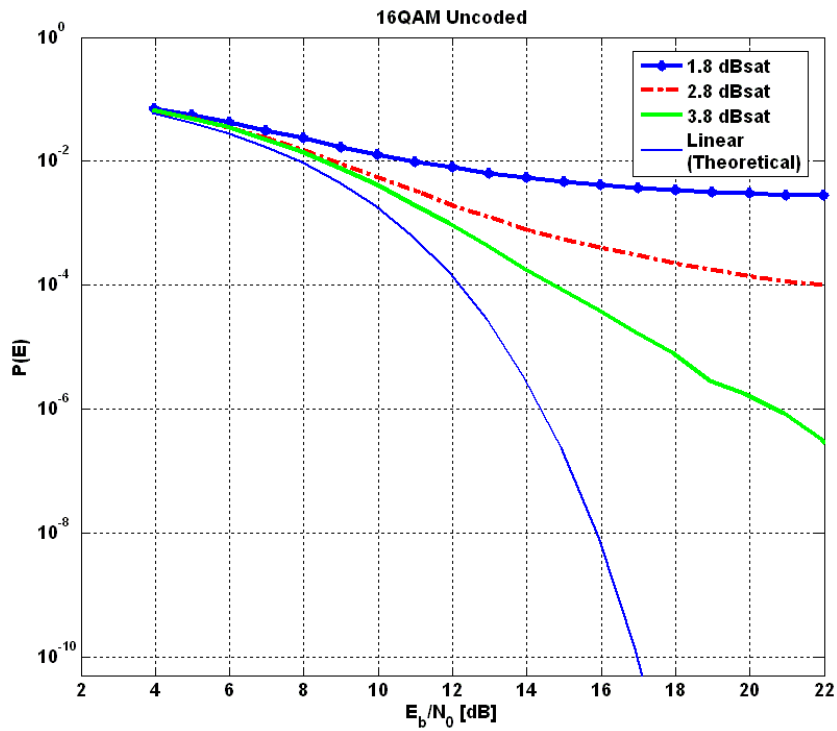
Figure 5.1: 8PSK Uncoded BER Plot
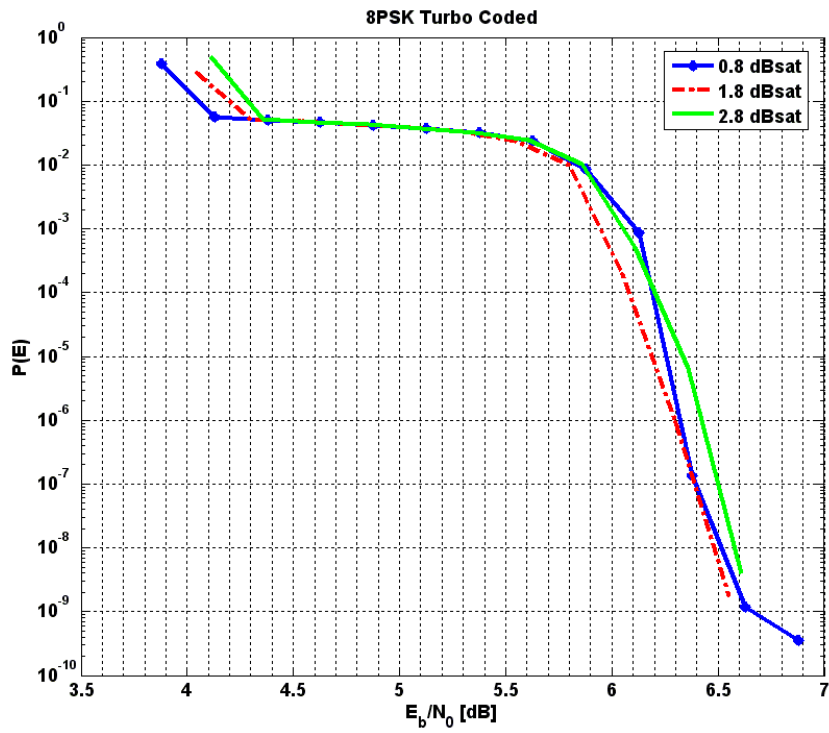

Figure 5.2: 16QAM Uncoded BER Plot

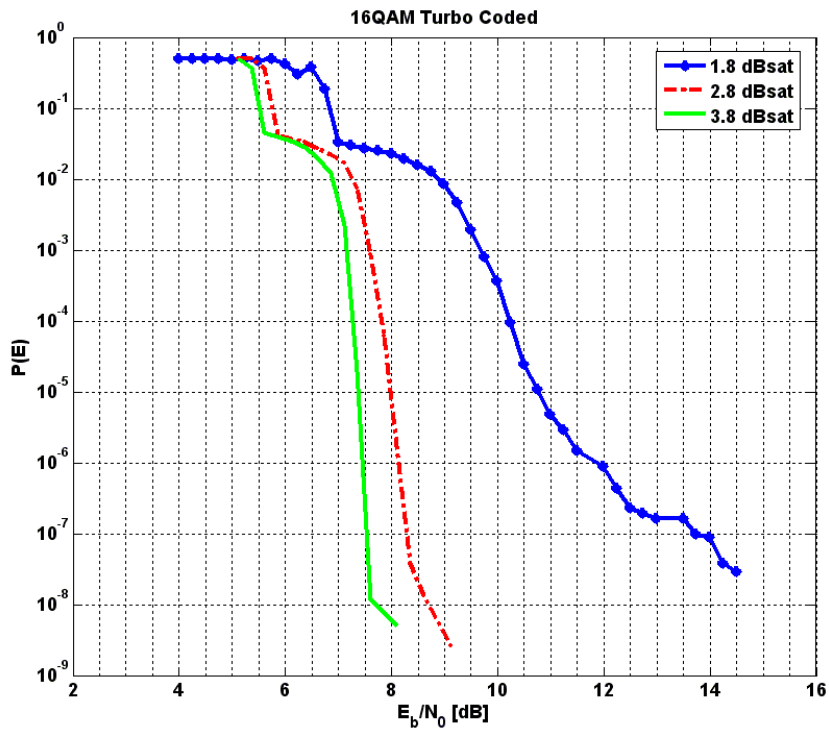Figure 5.3: 8PSK Coded BER Plot

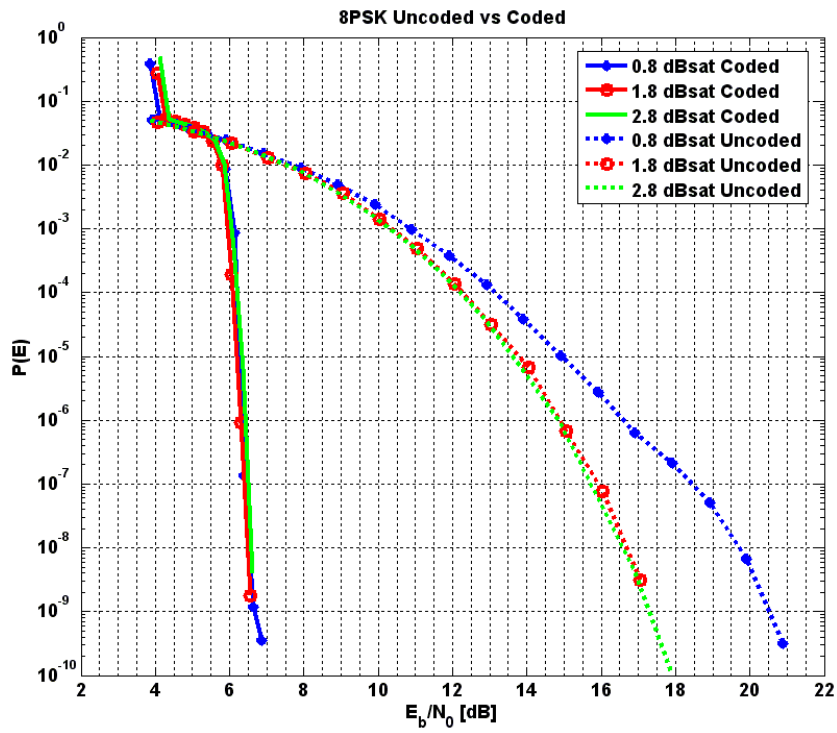

Figure 5.4: 16QAM Coded BER Plot
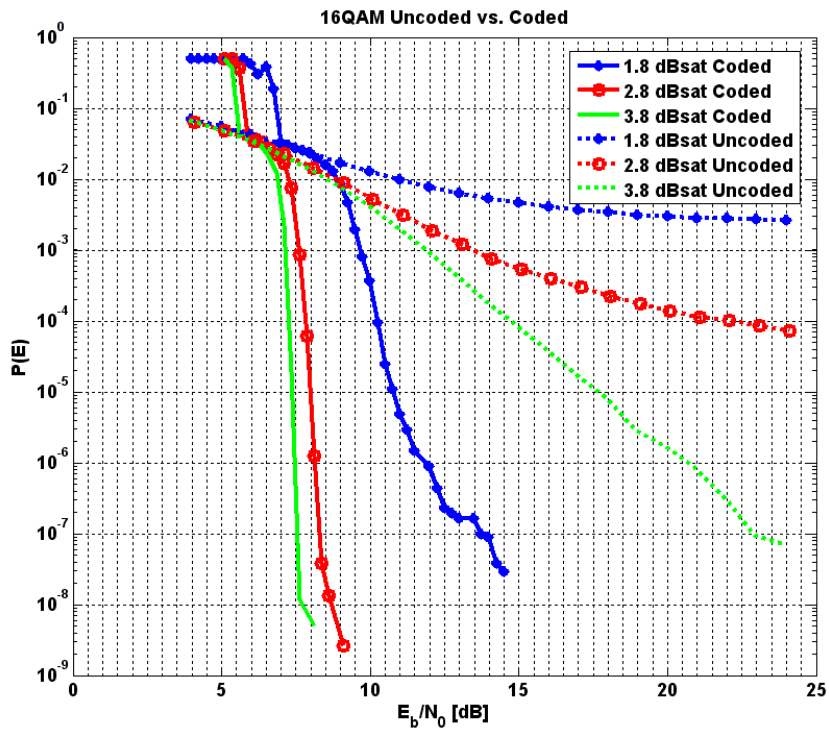
Figure 5.5: 8PSK Coded vs. Uncoded BER Plot

Figure 5.6: 16QAM Coded vs. Uncoded BER Plot

transmitting bits until 40 errors are obtained and from those 40 errors the bit error rate is calculated. It takes approximately 30 hours to obtain a turbo coded BER plot down to a rate of 10^{-9}. Uncoded BER plots require considerably less time.

Figures 5.1 and 5.2 depict the uncoded performance of 8PSK and 16QAM, respectively. It can be seen that the 16QAM modulation is more dramatically affected by nonlinearity than 8PSK. While at 1.8 dBsat in 16QAM, the BER does not go lower that 10^{-3}, 8PSK at 0.8 dBsat only has about a 4 dB loss at 10^{-8}.

Moving on to the coded BER plots, Figures 5.3 and 5.4 show the performance of 8PSK and 16QAM, respectively. Here, the nonlinear effect are even more noticeable. The coded BER plots of 8PSK are very similar, which shows that nonlinearities have little effect on the performance. On 16QAM the difference between each data line is significantly different.

Figures 5.5 and 5.6 combine the results of the previous plots into one plot. These plots demonstrate that the coding gain, as described in Figure 3.3 is easily established in the 8PSK modulation but not in 16QAM.

5.2.1   Coding Gain

Keeping in mind the objective of this work, the possibility of predicting the performance of turbo coding in nonlinear conditions based on the performance of turbo coding in linear conditions is now explored. Most literature and data sheets regarding the performance of coding algorithms (including turbo coding) uses the *coding gain* metric as the measure of their performance. Of course, this coding gain is generally measured in a linear environment.

The overall idea of coding is that an algorithm with particular mathematical properties is used in order to be able to correct some errors at the receiver end of the communications system. Therefore, it is reasonable to expect that a coding algorithm will be able to correct a predefined number of errors at a given signal-to-noise ratio (E_b/N_0), that is, to expect that there is a unique correspondence from uncoded BER to coded BER. For example, if there is a uncoded BER of 10^{-4} at 10 dB (E_b/N_0), turbo coding can give at BER of 10^{-7} at the same E_b/N_0 level. This means that turbo coding corrects 10^3 mistakes for every 10^7 transmitted

bits. If this is the case, then the sought ability to predict the performance of turbo coding in a nonlinear situation is possible by comparing the coding gains. The following set of plots show that this is not the case and that the coding gain of turbo coding is dependant on the level of nonlinearity and the unique correspondence previously mentioned does not emerge out of the results obtained.

Figures 5.7 and 5.8 describe the coding gain at each E_b/N_0 and the correspondence of uncoded BER to coded BER of 8PSK, respectively. Figures 5.9 and 5.10 provide the same information for 16QAM. It can be seen from these figures that coding gain and the mapping of uncoded BER to coded BER are very much dependent on the amount of nonlinearity added to the system. As the amplifier in the system approaches saturation, the plots of the coding gain and the BER mapping deviate more from the case of the linear system. If coding gain was independent from the effects of nonlinearities, the data lines in Figures 5.8 and 5.10 would be identical and this is not the case. It is also important to note that the 16QAM constellation is much more affected by the nonlinearity than the 8PSK constellations. This shows that a nonlinear amplifier affects not only the shape of the received constellation and the BER but also the coding gain of turbo coding. And not only that, it also has a higher effect in 16QAM coding gain than in 8PSK coding gain.

5.3   4+12 APSK Constellation

5.3.1   Description and Definition

The 4+12 APSK constellation was first proposed by De Gaudenzi et al. [RDGP02] as a way to improve the performance of satellite communication systems. In section 5.2, it is shown that the 8PSK constellation is less affected by a nonlinear amplifier than the 16QAM, primarily because of the shape of the constellation. In the 8PSK constellation all points have the same magnitude, so the shape remains even through nonlinearities (as shown in Figure 2.4) while 16QAM has four outer points that suffer greatly under nonlinearities. Given the

fact that a 16-point constellation (i.e. a 4-bit symbol) has potentially greater capacity than an 8-point constellation (i.e. a 4-bit symbol), De Gaudenzi et al. proposed this 4+12 APSK (also called 16APSK) because it has a double ring structure that makes it less susceptible to nonlinear distortion than 16QAM, but still has the 16 points. The signal space representation of 4+12APSK is shown on Figure 5.11.

The signal in the time domain can be represented as:

$$s(t) = \sqrt{P} \sum_{k=-\infty}^{\infty} R(\psi_k) e^{j\psi_k} g_r(t - kT_s)$$

where P is the power of the signal, $R(\psi_k) \in R_1, R_2 = 1, 1/2.7$, and $\psi_k \in \Psi_1^1, .., \Psi_{N_1}^1, \Psi_1^2, ..., \Psi_{N_2}^2$. R is the amplitude of the signal and ψ is the phase of the signal. g_r is the transmission impulse response and T_s is the symbol period [16].

5.3.2 Performance of 4+12 APSK

The performance of 4+12 ASPK is analyzed in [RDGM07]. All results found were obtained using a linear environment. The important findings from the work of De Gaudenzi et al. is that the performance of 4+12 APSK performs very close to 16QAM in a linear setting, but has a loss of about 0.5dB in the uncoded case and about 0.1dB in the coded case.

For this thesis, a computer simulation using MATLAB is created in order to obtain the expected performance of 4+12 APSK in the communication system described in Chapter 4. The 4+12 APSK performance must be simulated in software because the hardware platform, in particular the turbo encoder/decoder chip does not support this constellation. The computer simulation includes models of the following individual systems:

- Bit generator

- Turbo Encoder

- Digital Modulator

- Nonlinear Amplifier

- Noise Generator

- Digital Demodulator

- Turbo Decoder

The turbo encoder/decoder software used for this simulation is the AHA Galaxy Simulation Tool for MATLAB [AHA]. This toolkit includes the possibility to optimize some parameter of turbo coding. The parameters used are the same one as the ones used for the actual turbo coding ASIC used in the hardware system. The model of the nonlinear amplifier is obtained by experimental results of the input output relationships of the TWTA used in the hardware system. The nonlinear model considers both AM/AM distortion and AM/PM distortion.

The simulated model of the system is tested with the results obtained from the hardware platform using 16QAM and 8PSK to confirm accuracy. On average, the simulated model results are off from the hardware platform results by no more that 0.2 dB.

Finally, using this simulated model, the performance of the turbo coded 4+12 APSK constellation is compared to turbo coded 16QAM.

Previous works have shown that the 4+12 APSK constellation has a similar performance to 16QAM when coded in a linear environment [RDGM07]. Because 4+12 APSK is known to be a more robust constellation when dealing with nonlinear channels when no coding algorithm is used, it was expected that the coded 4+12 APSK constellation through a nonlinear channel would provide better performance. The work of this thesis shows that that is the case as seen in Figure 5.12. This figure shows the performance of 4+12 APSK and 16QAM. Both constellations are submitted to a nonlinearity of 1.8 dBsat and they include turbo coding. The BER plot of 4+12 APSK displays lower BER than 16QAM. At a BER of 10^{-4}, APSK shows a gain of about 1.5 dB.
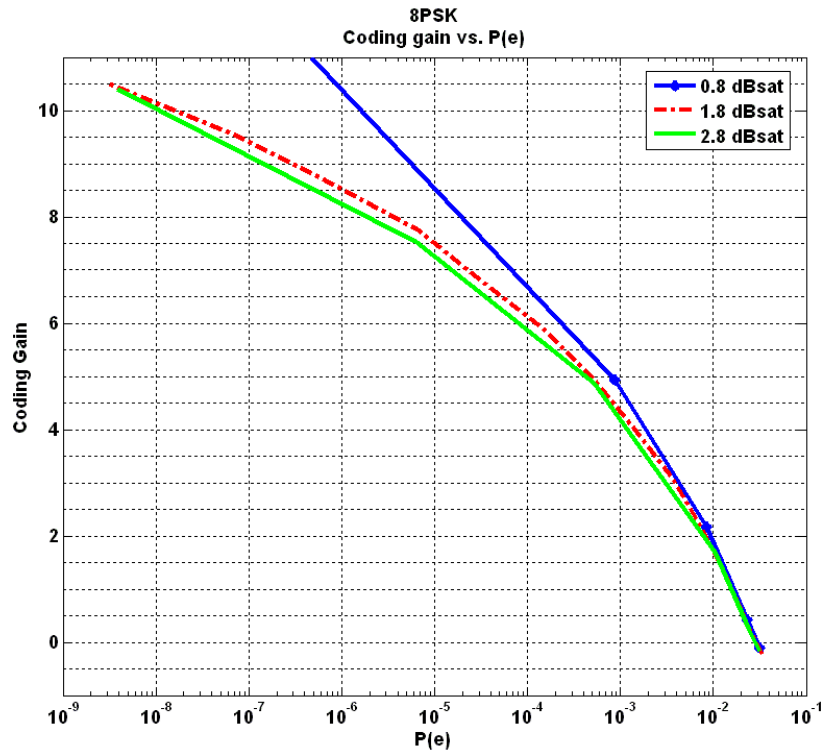
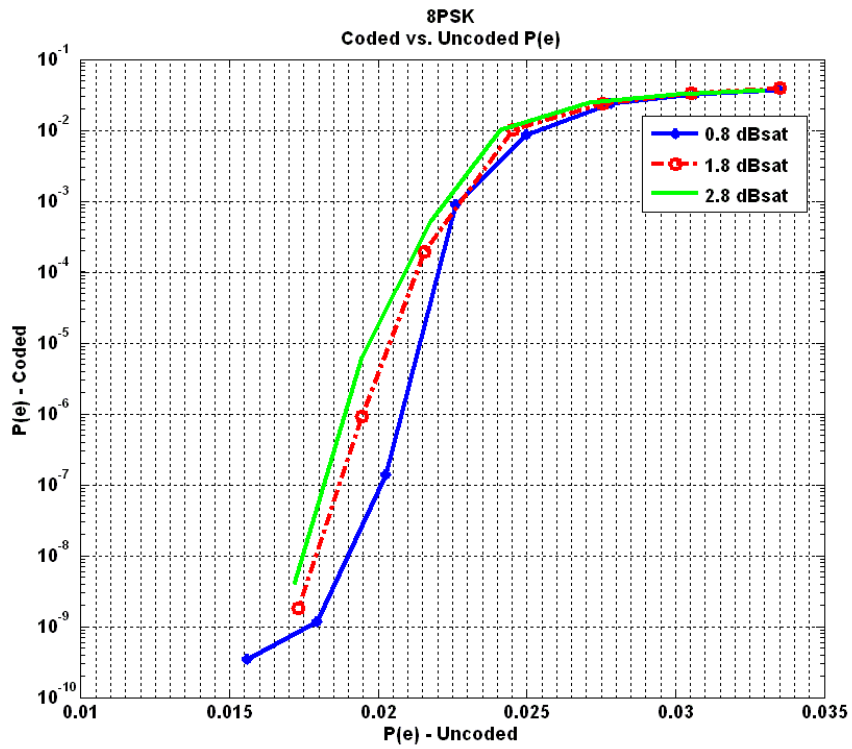Figure 5.7: Coding gain of 8PSK at different power levels

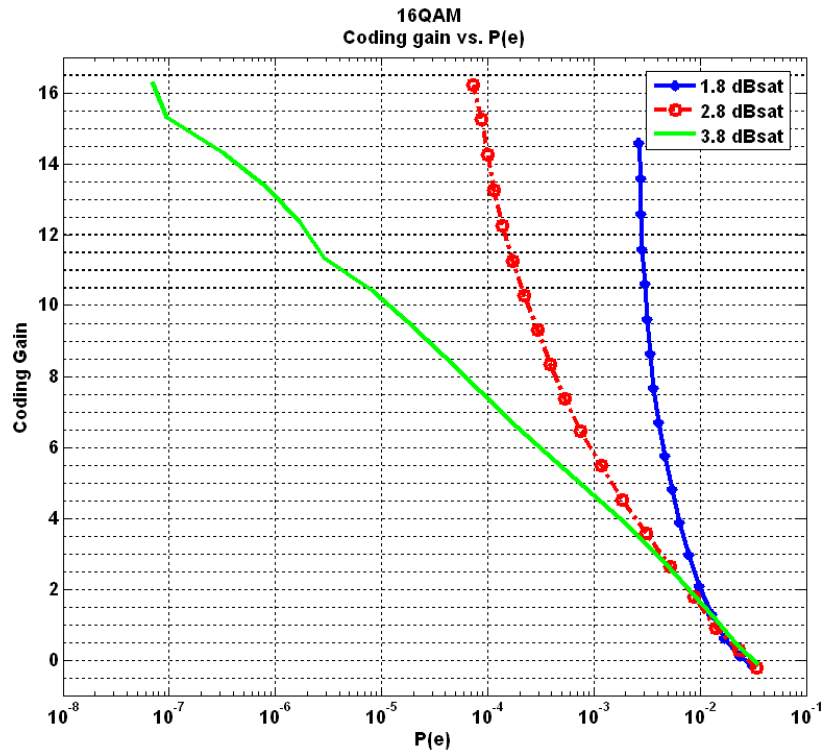Figure 5.8: BER mapping of 8PSK at different power levels

Figure 5.9: Coding gain of 16QAM at different power levels
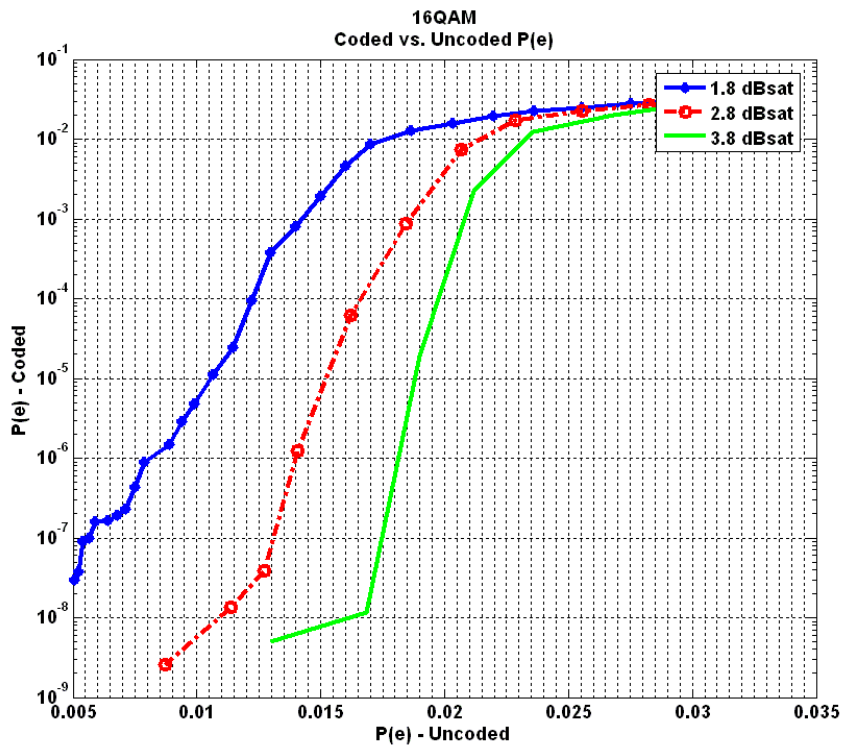

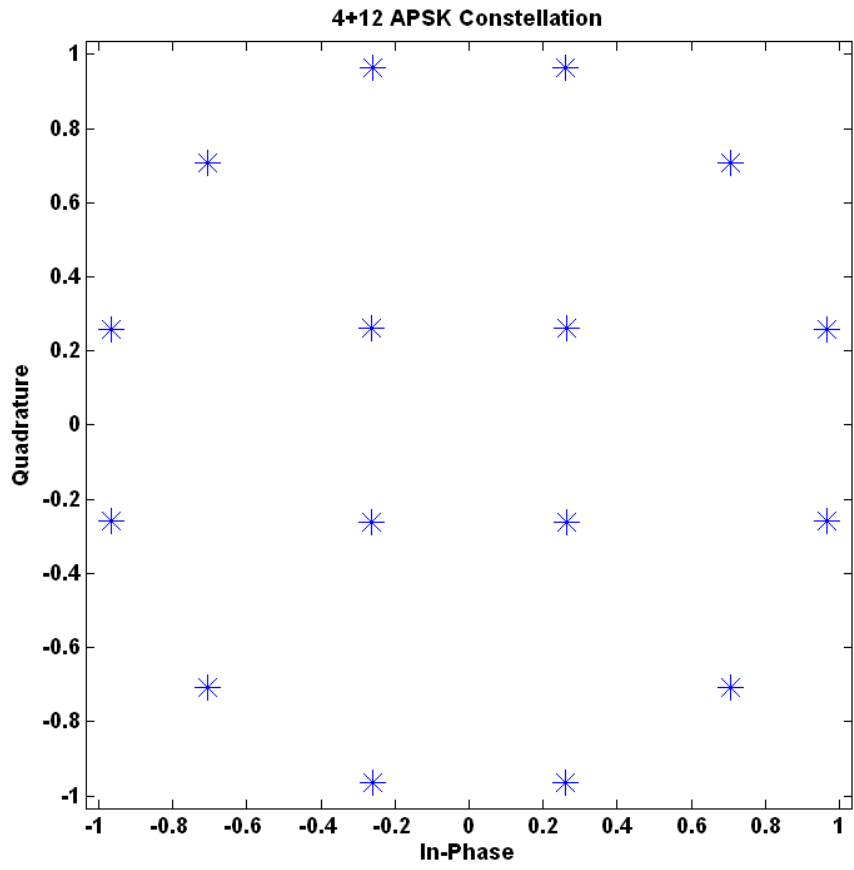Figure 5.10: BER mapping of 16QAM at different power levels
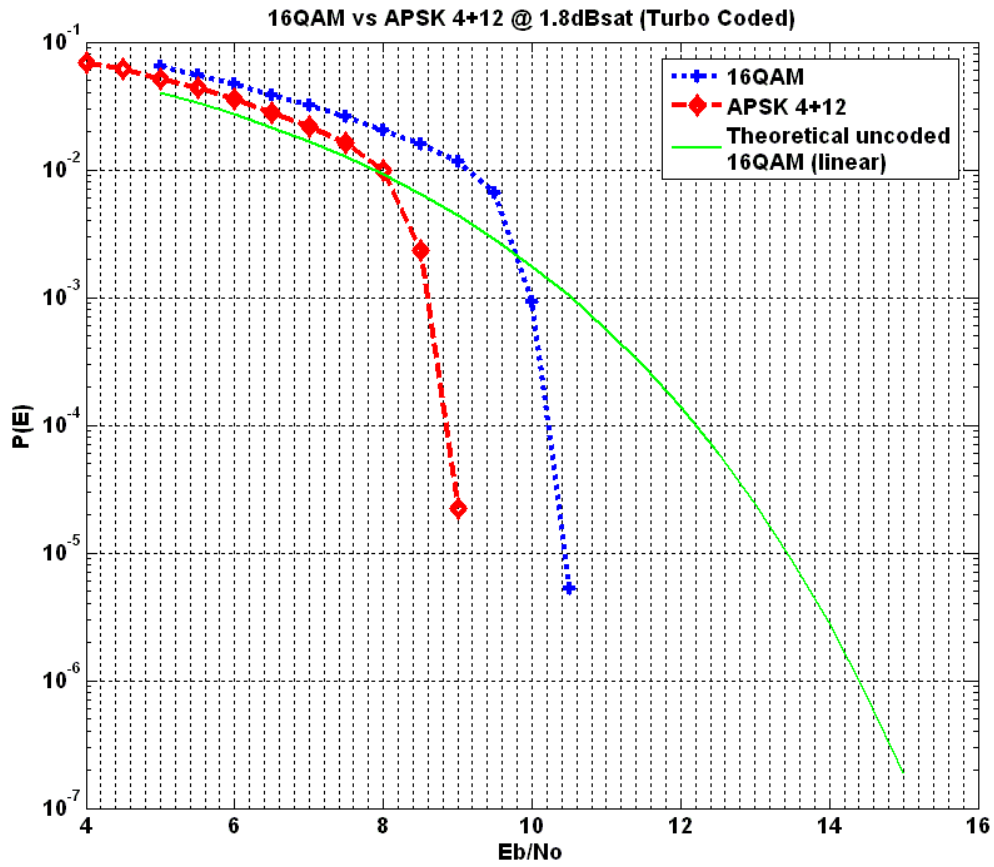
Figure 5.11: Signal space representation of 4+12 APSK

Figure 5.12: Coded performance of coded 16QAM and 4+12 APSK @ 1.8dBsat

Chapter 6

Conclusions and Future Work

6.1 Conclusions

The objective of this thesis is to provide a comprehensive analysis of the behavior of turbo coding in a nonlinear environment. To achieve this objective, a wide range, multi-parameter set of bit error rate plots was constructed and analyzed. Also, the novel 4+12 APSK modulation scheme was examined. The research performed showed two major results that provide a deeper insight into this subject.

First, the analysis of the BER performance of the system with different parameter showed that coding gain of turbo codes is dependant on the level of nonlinearity. Contrary to what might have been expected, there is no unique correspondence between uncoded BER and coded BER, that is to say that turbo code do not fix a specific number of errors. The possible explanation for this phenomenon is the fact that turbo codes works with soft decision algorithms and therefore its ability to correct errors depends on how incorrect the error is. Nonlinearities change the shape of the constellation and thus make the errors be more difficult to correct.

The other major result is the demonstration of the better performance of turbo coded 4+12 APSK than turbo coded 16QAM in a nonlinear environment. This shows that the expected behavior is actually the case. The 4+12 APSK constellation is better suited for nonlinear channels than 16QAM because of its double ring structure. The turbo coded constellation in a nonlinear environment was shown to have a better BER performance that 16 QAM.

6.2   Future Work

As a result of this research, several possibilities for future work and improvements surfaced. It would be very beneficial to perform the same analysis performed here with turbo coding using some other type of coding algorithm that uses hard decisions on all its process to determine if that is the factor that makes the coding algorithm dependent on the nonlinearity.

Also, given the results of the performance of the 4+12 APSK modulation scheme, a customized ASIC capable of supporting this scheme could be fabricated and implemented in the actual hardware system to obtain real hardware results that would be not only more reliable, but obtained in a fraction of the time required in software simulation.

Finally, a further issue to be explored is the concept of the optimal way to scale a received signal after a nonlinearity in order to acquire the best performance out the system. This issue arose in this work from the simulation of the model of the nonlinear amplifier. The average power method was used in this work but the possibility of a better performing algorithm exists.

References

[AHA]   AHA, Pullman, WA. *AHA Galaxy: Simulation Tool Kit User's Guide*.

[BM96]   Sergio Benedetto and Guido Montorsi. Unveiling turbo codes: Some results on parallel concatenated coding schemes. *IEEE Trans. Inf. Theory*, 42(2):409–428, March 1996.

[CBT93]   A. Glavieux C. Berrou and P. Thitimajshima. Near shannon limit error-correcting coding and decoding: Turbo-codes. , *IEEE International Conference on Communications*, 2:1064 – 1070, May 1993.

[Com05]   Comtech AHA Group, Moscow, ID. *AHA4541 Product Brief*, 2005.

[GD05]   Eugene Grayver and Phillip Dafesh. Multi-modulation programmable transceiver system with turbo coding. In *IEEE Aerospace Conference Proceedings*, pages 1–10, Big Sky, MT, May 2005.

[GS06]   E. Grayver and P. E. Santacruz. Effects of nonlinear amplification on turbo coding. In *IEEE Aerospace Conference Proceedings*, Big Sky, MT, May 2006.

[HG02]   J. Hagenauer and N. Gortz. The turbo principle in joint source-channel coding. In *IEEE Information Theory Workshop*, pages 1398 – 1402, May 2002.

[LJ04]   Shu Lin and Daniel J. Costello Jr. *Error Control Coding*. Pearson Prentice Hall, Upper Saddle River, NJ, 2004.

[MDA03]   Kambiz Madani Markus Dillinger and Nancy Alonistioti. *Software Radio: Architecture, Systems and Functions*. Wiley, Hoboken, NJ, 2003.

[Pro01]   John G. Proakis. *Digital Communications*. McGraw-Hill, New York, 2001.

[RDGM07] Albert Guillen i Fabregas Riccardo De Gaudenzi and Alfonso Martinez. Turbo-coded apsk modulations for satellite broadband communications - part i: Coded modulation design. *IEEE Transactions on Wireless Communications*, 2007.

[RDGP02] A. Martinez R. De Gaudenzi, A. Fabregas and B. Ponticelli. A novel high power and spectral efficient coded modulation for nonlinear satellite channels. In *AIAA International Communication Satellite Systems Conference and Exhibit*, Montreal, Quebec, May 2002.

[Rod01] Dennis Roddy. *Satellite Communications*. McGraw-Hill, New York, 2001.

[Sha48] Claude E. Shannon. A mathematical theory of communication. *The Bell System Technical Journal*, 27:379–423, 623–656, October 1948.

[tB01] S. ten Brink. Convergence behavior of iteratively decoded parallel concatenated codes. *IEEE Trans. Communications*, 49(10):1727 – 1737, October 2001.

[VY00] Branka Vucetic and Jinhong Yuan. *Turbo Codes*. Kluwer Academic Publishers, Boston, MA, 2000.

[XIL05] XILINX. *Virtex-II Platform FPGAs: Complete Data Sheet*, v3.4 edition, March 2005.

Curriculum Vitae

Pedro Enrique Santacruz was born on June 29, 1982. The first son of Jesus Enrique Santacruz and Eustacia Santacruz, he graduated as Valedictorian from Mountain View High School, El Paso, Texas, in the spring of 2000. In the fall of 2000 he entered The University of Texas at El Paso. From 2000 to 2004 he pursued his Bachelor's Degree in Electrical Engineering and was involved in different organizations including the Institute of Electrical and Electronics Engineers (IEEE), Mexican American Engineers and Scientists (MAES), Tau Beta Pi, and Eta Kappa Nu. In spring 2004, he received the Bachelor of Science degree in Electrical Engineering Summa Cum Laude and was recognized as the Student Marshal for the College of Engineering during the Commencement ceremony. In fall 2004 Pedro began graduate studies at The University of Texas at El Paso as a fellow of the National Consortium for Graduate Degrees for Minorities in Engineering and Science (GEM). He interned with The Aerospace Corporation during the summers of 2004 and 2005. In 2005, he received a Bridge to the Doctorate Fellowship from the Louis Stokes Alliance for Minority Participation (LSAMP). In the fall of 2006 Pedro will begin pursuing a Ph.D. at Rice University.

Permanent address: 3799 Judy Marie

El Paso, Texas 79938

This thesis was typed by the author.